



University of Kentucky
UKnowledge

Plant and Soil Sciences Faculty Publications

Plant and Soil Sciences

8-15-2021

Nitrogen and Rainfall Effects on Crop Growth—Experimental Results and Scenario Analyses

Saadi Sattar Shahadha
Al-Karkh University of Science, Iraq

Ole O. Wendroth
University of Kentucky, owendroth@uky.edu

Dianyuan Ding
Yangzhou University, China

Follow this and additional works at: https://uknowledge.uky.edu/pss_facpub

 Part of the [Plant Sciences Commons](#), and the [Soil Science Commons](#)

[Right click to open a feedback form in a new tab to let us know how this document benefits you.](#)

Repository Citation

Shahadha, Saadi Sattar; Wendroth, Ole O.; and Ding, Dianyuan, "Nitrogen and Rainfall Effects on Crop Growth—Experimental Results and Scenario Analyses" (2021). *Plant and Soil Sciences Faculty Publications*. 162.

https://uknowledge.uky.edu/pss_facpub/162

This Article is brought to you for free and open access by the Plant and Soil Sciences at UKnowledge. It has been accepted for inclusion in Plant and Soil Sciences Faculty Publications by an authorized administrator of UKnowledge. For more information, please contact UKnowledge@lsv.uky.edu.

Nitrogen and Rainfall Effects on Crop Growth—Experimental Results and Scenario Analyses

Digital Object Identifier (DOI)

<https://doi.org/10.3390/w13162219>

Notes/Citation Information

Published in *Water*, v. 13, issue 16, 2219.

© 2021 by the authors. Licensee MDPI, Basel, Switzerland.

This article is an open access article distributed under the terms and conditions of the Creative Commons Attribution (CC BY) license (<https://creativecommons.org/licenses/by/4.0/>).

Article

Nitrogen and Rainfall Effects on Crop Growth—Experimental Results and Scenario Analyses

Saadi Sattar Shahadha ^{1,*}, Ole Wendroth ² and Dianyuan Ding ³ ¹ College of Energy and Environmental Sciences, Al-Karkh University of Science, Baghdad 10081, Iraq² Department of Plant & Soil Sciences, University of Kentucky, 1100 Nicholasville Road, Lexington, KY 40506, USA; owendroth@uky.edu³ College of Hydraulic Science and Engineering, Yangzhou University, Yangzhou 225009, China; dyding@yzu.edu.cn

* Correspondence: saadishahadha@kus.edu.iq

Abstract: Nitrogen (N) fertilization is critical for crop growth; however, its effect on crop growth and evapotranspiration (ET_c) behaviors under different amounts of rainfall is not well understood. As such, there is a need for studying the impact of nitrogen application rates and rainfall amounts on crop growth and ET_c components. Agricultural system models help to fill this knowledge gap, e.g., the Root Zone Water Quality Model (RZWQM2), which integrates crop growth-related processes. The objective of this study is to investigate the effect of the nitrogen application rate on crop growth, soil water dynamics, and ET_c behavior under different rainfall amounts by using experimental data and the RZWQM2. A field study was conducted from 2016 to 2019 with three nitrogen application rates (0, 70, and 130 kg N ha⁻¹) for unirrigated winter wheat (*Triticum aestivum* L.), and two nitrogen application rates (0 and 205 kg N ha⁻¹) for unirrigated corn (*Zea mays* L.). For the period of 1986–2019, the amounts of actual rainfall during each crop growth period are categorized into four groups. Each rainfall group is used as a rainfall scenario in the RZWQM2 to explore the interactions between the rainfall amounts and N levels on the resulting crop growth and water status. The results show that the model satisfactorily captures the interaction effects of nitrogen application rates and rainfall amounts on the daily ET_c and soil water dynamics. The nitrogen application rate showed a noticeable impact on the behavior of soil water dynamics and ET_c components. The 75% rainfall scenario yielded the highest nitrogen uptake for both crops. This scenario revealed the highest water consumption for wheat, while corn showed the highest water uptake for the 100% rainfall scenario. The interaction between a high nitrogen level and 50% rainfall yielded the highest water use efficiency, while low nitrogen and 125% rainfall yielded the highest nitrogen use efficiency. A zero nitrogen rate yielded the highest ET_c and lowest soil water content among all treatments. Moreover, the impacts of the nitrogen application rate on ET_c behavior, crop growth, and soil water dynamics differed depending on the received rainfall amount.

Keywords: nitrogen application rate; rainfall amount; soil water dynamics; evapotranspiration; crop growth; water/nitrogen use efficiency



Citation: Shahadha, S.S.; Wendroth, O.; Ding, D. Nitrogen and Rainfall Effects on Crop Growth—Experimental Results and Scenario Analyses. *Water* **2021**, *13*, 2219. <https://doi.org/10.3390/w13162219>

Academic Editor: Holger Rupp

Received: 6 July 2021

Accepted: 10 August 2021

Published: 15 August 2021

Publisher's Note: MDPI stays neutral with regard to jurisdictional claims in published maps and institutional affiliations.



Copyright: © 2021 by the authors. Licensee MDPI, Basel, Switzerland. This article is an open access article distributed under the terms and conditions of the Creative Commons Attribution (CC BY) license (<https://creativecommons.org/licenses/by/4.0/>).

1. Introduction

The sustainable management of nitrogen is challenging [1,2] due to the complex transformation dynamics of nitrogen (N) in soil. N fertilization can affect the available water in soil through increased plant transpiration as a consequence of increased plant canopy development. When soil water is limited during the flowering stage, nitrogen use efficiency can be substantially decreased [3–5].

Crop yields and growth greatly depend on applied N and the availability of soil water [6]. In many studies, the effects of N fertilization on crop growth, yield formation, and nitrogen use efficiency have been reported [7,8]. In [9], the water–nitrogen interactions during a wheat growing season using three irrigation treatments (2, 3, and 4 irrigations

per growing season) and several N levels were considered for evaluating the performance of the CERES-Wheat and CropSyst models. In [10], actual evapotranspiration during vegetative and reproductive maize growth periods was evaluated for different nitrogen treatments under full and limited irrigation. It was found that N fertilizer applied during the reproductive period increased the actual evapotranspiration (ETc). In [11], the impact of nitrogen–water interaction on maize growth for silage using several nitrogen and irrigation rates was studied. It was found that an onset of irrigation when the available soil water storage was depleted to 85% was the optimum irrigation timing for maize at the study site. Additionally, the effects of different N application rates on crop growth, water use efficiency, and ETc for irrigated and rainfed crops have been quantified in several other studies [6,12–14].

In previous studies, the amounts of applied water (irrigation/rainfall) have not been excessive. It is critical to understand the impacts of excessive irrigation/rainfall on crop growth, soil water dynamics, and evapotranspiration behaviors, as well as the interactions between the amount of applied N fertilizer and application timing. The interaction impacts of different nitrogen rates and excessive rainfall amounts on crop growth and water status are not sufficiently understood. In particular, crop ETc behavior over the entire growing season is not well understood. It is still challenging to quantify the interaction effects of soil water and nitrogen availability on the ETc behavior, particularly its components, i.e., crop transpiration and soil evaporation. Studying the impacts of excessive rainfall amount on the soil nitrogen status and the effect on crop ETc is indispensable for the development of sustainable crop field management.

Agricultural system models which integrate many related processes are good tools to quantify the impacts of N fertilization rates on soil water dynamics, ETc, and crop growth under different rainfall amounts over a growing season. The Root Zone Water Quality Model is one of the most widely used agricultural system models. The model can simulate the effects of management practices, weather, and soil properties on water dynamics and crop growth [15–18]. In [19], the RZWQM was evaluated under different nitrogen management strategies for applying mineral N and manure. Satisfactory model simulations for the corn yield, N loss, and soil N concentrations were obtained with $R^2 > 0.80$ and RMSE $< 20\%$. The work in [20] also simulated the crop evapotranspiration, soil water content, and leaf area index with RMSE values of 1.4 mm, $0.046 \text{ m}^3/\text{m}^3$, and 1.1, respectively, for winter wheat when using the RZWQM. The work in [21] used the RZWQM to evaluate and develop nitrogen and water management strategies for winter wheat under different N treatments. The RZWQM was useful for simulating the soil water content, crop growth, and plant N uptake. Additionally, RZWQM2 performed satisfactorily when simulating the effects of climate change and elevated atmospheric CO_2 concentrations on water and nitrogen dynamics, in addition to crop growth after calibrating the measured soil hydraulic properties as input parameters [22]. The work in [23] also successfully simulated the effects of the climate, initial soil water levels at planting, frequencies, amounts of irrigation, and N rates in terms of water and nitrogen efficiency. The best management practice for obtaining an optimum corn grain yield was found with irrigation scheduled at every 3 to 7 days to cover 90% ET losses and an N fertilization rate of 200 kg ha^{-1} ; however, the interactions between N application rates and excessive rainfall amounts and the influences on soil water dynamics and ETc behaviors have not been studied. As such, the objective of this study is to explore the interactions between N application rates and rainfall amounts on ETc behaviors, water and nitrogen use efficiency, and crop growth during a growing season for wheat and corn through the use of RZWQM2.

2. Materials and Methods

2.1. ET Simulation in the RZWQM2

The RZWQM2 model has been described in detail in [6,15,24–29]. Consequently, this study is focused on the critical information related to the ETc simulations. The actual crop evapotranspiration simulated by RZWQM2 is a sum of actual soil evaporation and actual

crop transpiration [15]. Actual soil evaporation is calculated using Richards' soil water movement equation by assuming that the evaporative demand is equal to the potential evaporation rate at the soil surface [30]. Actual crop transpiration is computed by an empirical root water uptake equation [31] that is not allowed to exceed the potential plant transpiration. The potential soil evaporation/crop transpiration rates are obtained from the extended Shuttleworth–Wallace model [31] ET model [32]. For estimating ETc, the resistances in the soil and canopy residue system caused by crop residues are included by the extended Shuttleworth–Wallace model [32], which is a double layer version of the Penman–Monteith equation [33]:

$$\lambda ET = CC(PM_c) + CS(PM_s) + CR(PM_r) \quad (1)$$

where λET is the total flux of latent heat above the canopy and PM_c , PM_s , and PM_r are the Penman–Monteith equations applied to the canopy, bare soil, and residues, respectively. CC , CS , and CR are coefficients based upon the fractions of the area covered by the canopy, bare soil, and residue, respectively.

Equation (1) covers three possible scenarios: First, if no surface residue is present, CR will be zero, and Equation (1) consequently reduces to the original Shuttleworth–Wallace model. The second scenario represents the absence of a crop, with the consequence that CC will be zero and Equation (1) will be a Penman–Monteith type soil evaporation model. In the third scenario, when the canopy is completely covering the field, CS and CR are zero, and Equation (1) becomes the original Penman–Monteith model. Details about the CC , CR , and CS terms can be found in [34].

In this model, there are several possible scenarios of resistance against evapotranspiration [35]: First, soil surface resistance (r_s^c), which is the soil surface resistance to evaporate soil water and increases as the soil surface dries [36]. Second, canopy resistance is composed of the mean canopy boundary layer resistance, r_a^c , and bulk stomatal resistance, r_s^c , which is the canopy resistance in the Penman–Monteith equation. It is affected by the substomatal cavities and boundary layer around the leaves [37,38]. The mean canopy boundary layer resistance, r_a^c , is calculated in the Shuttleworth–Wallace model as follows:

$$r_a^c = \frac{r_b}{(2LAI)} \quad (2)$$

where $r_b/2$ is the mean leaf boundary layer resistance of amphistomatous leaves per unit surface area of vegetation and LAI is the leaf area index.

The bulk stomatal resistance is calculated as follows:

$$r_s^c = \frac{r_s}{(2LAI)}, \text{ for } LAI \leq 2 \quad (3)$$

$$r_s^c = \frac{r_s}{(LAI)}, \text{ for } LAI > 2 \quad (4)$$

where $r_s/2$ is the mean stomatal resistance of amphistomatous leaves and r_s^c decreases with increasing the LAI without restrictions.

Most plant leaves contribute to the transpiration process at LAI values less than three [39]; however, the LAI_{eff} decreases as the canopy develops and LAI becomes higher than 3 [33,40]. A LAI increase of three or larger becomes a non-limiting factor for evapotranspiration. In such cases, the transpiration rate becomes independent of LAI as long as the soil water is not limiting the transpiration rate [41]. The LAI_{eff} for the entire range of LAI in the RZWQM2 model is estimated as follows:

$$LAI_{eff} = LAI \text{ for } LAI \leq 1 \quad (5)$$

$$LAI_{eff} = 0.5LAI \text{ for } LAI \geq 3 \quad (6)$$

$$LAI_{eff} = LAI(1.25 - 0.25LAI) \text{ for } 1 \leq LAI \leq 3 \quad (7)$$

2.2. Experimental Design and Measurements

The experiment detailed in this work was conducted at the University of Kentucky Spindletop Research Farm, Lexington, Kentucky. The experiment was performed in a humid subtropical (Köppen Cfb) climate with an average annual precipitation of 114 cm and a mean annual temperature of 13 °C. The soil was a Maury silt loam, classified as a mixed, semiactive, mesic Typic Paleudalf [42].

A soil profile was opened for collecting disturbed and undisturbed soil samples at five soil depths of 0–10, 20–30, 40–50, 60–70, and 80–90 cm. At each depth, three replicates of soil core cylinders and disturbed samples were collected for measuring the soil water retention curve, unsaturated hydraulic conductivity, soil texture, and bulk density. Saturated hydraulic conductivity (Ksat) was measured in the field with a borehole permeameter (Soil Measurement Systems) [43] at five depths (10, 30, 50, 70, and 90 cm) with two replicates per depth (Table 1). In addition, the soil organic matter (SOM), total nitrogen (N), soil organic carbon (SOC) contents, C/N ratio, pH, base saturation (B.S.), NO₃, NH₄-N concentration, and cation exchange capacity (CEC) were quantified at depths of 0–15, 15–30, 30–60, and 60–90 cm during crop development and maturity stages (Table 2).

Table 1. Field measurements and model inputs of soil physical and hydraulic properties.

Field Measurements								
Soil horizon	Particle fraction (%)			Bulk density	Ksat	Θ at 0.10 bar	Θ at 0.33 bar	Θ at 15 bar
(cm)	Sand	Silt	Clay	(g/cm ³)	(cm/h)	(cm ³ /cm ³)	(cm ³ /cm ³)	(cm ³ /cm ³)
0–10	0.07	0.70	0.23	1.46	0.44	0.37	0.33	0.19
20–30	0.06	0.64	0.30	1.39	0.95	0.35	0.33	0.23
40–50	0.06	0.55	0.39	1.48	0.13	0.39	0.37	0.27
60–70	0.08	0.43	0.49	1.40	0.30	0.42	0.39	0.30
80–90	0.09	0.35	0.56	1.37	1.20	0.43	0.40	0.33
After calibration								
Soil horizon	Particle fraction (%)			Bulk density	Ksat *	Θ at 0.10 bar	Θ at 0.33 bar	Θ * at 15 bar
(cm)	Sand	Silt	Clay	(g/cm ³)	(cm/h)	(cm ³ /cm ³)	(cm ³ /cm ³)	(cm ³ /cm ³)
0–10	0.07	0.70	0.23	1.45	0.50	0.35	0.28	0.14
10–20	0.08	0.70	0.22	1.45	0.65	0.37	0.30	0.15
20–30	0.06	0.64	0.30	1.40	0.60	0.41	0.34	0.19
30–40	0.06	0.61	0.33	1.43	0.50	0.39	0.34	0.23
40–50	0.06	0.55	0.39	1.45	0.40	0.39	0.35	0.24
50–60	0.07	0.49	0.44	1.43	0.40	0.40	0.36	0.26
60–70	0.08	0.43	0.49	1.40	0.45	0.42	0.38	0.27
70–80	0.09	0.38	0.53	1.37	0.50	0.41	0.38	0.29
80–90	0.09	0.35	0.56	1.37	0.80	0.42	0.39	0.30
90–150	0.09	0.30	0.61	1.36	0.70	0.42	0.39	0.30

* Black values are fixed while green values are calibrated. Ksat is the saturated hydraulic conductivity. Θ is the volumetric water content.

Table 2. Selected measured chemical properties of the soil profile before applying the N rates.

Soil Horizon (cm)	%SOM	% N	%SOC	pH	%B.S.	CEC (meq/100 g)	NO ₃ (kg/ha)	NH ₄ (kg/ha)
0–15	2.6	0.2	1.5	4.7	65.4	16	1.5	2.2
15–30	1.9	0.1	1.1	5	72.3	15.8	0.8	1.5
30–60	0.8	0.1	0.5	4.8	70.9	18.3	1	0.7
60–90	0.6	0.1	0.4	4.7	67.2	21.7	3	0.4

Winter wheat (*Triticum aestivum* L.) was planted on 2 November 2016 and harvested on 27 June 2017. It was grown in plots of 35 m by 5 m in with corn residue and without tilling. The experiment consisted of three N fertilizer rates with four replications. The N

fertilizer was applied as a liquid fertilizer with a farm sprayer. The N fertilizer rates were 0 (zero N), 70 (low N), and 130 (high N) kg N ha⁻¹. The fertilizer was applied as urea ammonium nitrate, which has 32% N in equal fractions of urea, ammonium, and nitrate. The 70 and 130 kg N ha⁻¹ rates were split across two applications. The first application occurred on March 13, 2017 and the second application occurred on 29 March 2017.

Corn (AgriGold A6499) was planted on 15 May 2019 with a row spacing of 76 cm and a population of 87,719 seeds per hectare. The corn was harvested on 18 September 2019. The corn was grown in plots of 35 m by 5 m with soybean residue and without tilling. The experiment consisted of two N fertilizer rates with three replications. The N fertilizer was applied as a liquid fertilizer with a farm sprayer. The N fertilizer rates were 0 (zero N) and 205 (high N) kg N ha⁻¹. The fertilizer was applied as urea ammonium nitrate. The 205 kg N ha⁻¹ rates were split across two applications. The first application occurred on 22 May 2019 (78 kg N ha⁻¹) and the second application took place on 5 June 2019 (127 kg N ha⁻¹).

The crop leaf area index (LAI) was measured about once a week with a LI-COR LAI-2000 Plant Canopy Analyzer during the development and maturity stages over the growing season (early March until harvesting). Six measurements were taken for each treatment at each LAI measurement time. Each measurement consisted of two readings above the canopy and four below the canopy and near the ground surface.

Soil water content was measured about once a week at 10 cm depth increments down to a 100 cm depth at the center of each plot using a capacitance probe (Diviner 2000, Sentek Pty Ltd., Stepney, South Australia). Soil water flux (SWF) across the 90 cm plane, i.e., the horizontal center of the 80–90 and 90–100 cm depth compartment, was quantified using Darcy's law for the days of measured soil water content. The SWF is the amount of water that is either lost across the lower boundary out of the root zone profile as deep drainage or gained through upward capillary rise into the root zone.

The daily average actual crop evapotranspiration was measured over approximately 7-day periods using the soil water balance method (SWB). The SWB method is based on the conservation of water mass within the root zone and has been widely used to estimate the actual crop evapotranspiration due to its accuracy [44–46].

Daily solar radiation, air temperature, rainfall, wind speed, and relative humidity were recorded at the research field with an ET107 weather station (Campbell Scientific Inc., Logan, UT 84321, USA) Lexington KY, USA. Weather data were used as RZWQM2 inputs (Figure 1). The weather data have been measured at a high resolution of ten minutes and were entered into the RZWQM2 with a daily resolution.

In addition to the nitrogen application rates (0, 70, and 130 kg/ha for the wheat and 0 and 200 kg/ha for the corn), four scenarios of rainfall were created during the model simulation to study the impacts of the nitrogen rates on the simulated soil water dynamics and crop evapotranspiration under different amounts of rainfall. These scenarios were categorized based on the actual rainfall fluctuation in the study area during the period of 1986 to 2019 (Figure 2). The rainfall scenarios (125%, 100%, 75%, and 50%) were created in the RZWQM2 by multiplying the actual rainfall of each growing season (wheat and corn) by 1.25, 1.00, 0.75, and 0.50, respectively. For example, when the rainfall of the wheat growing season 2016–2017 (1369 mm) was multiplied by 50%, the result was (698 mm), which is very close to the rainfall of the 2001–2002 wheat growing season (Figure 2). This means each one of the rainfall scenarios could be an actual rainfall for several years of the period of 1986–2019. Figure 2 shows that the rainfall obviously increased during the last few years, which is probably due to climate change. These rainfall changes need special attention to achieve appropriate understanding and devise an adaptation strategy for further climate change.

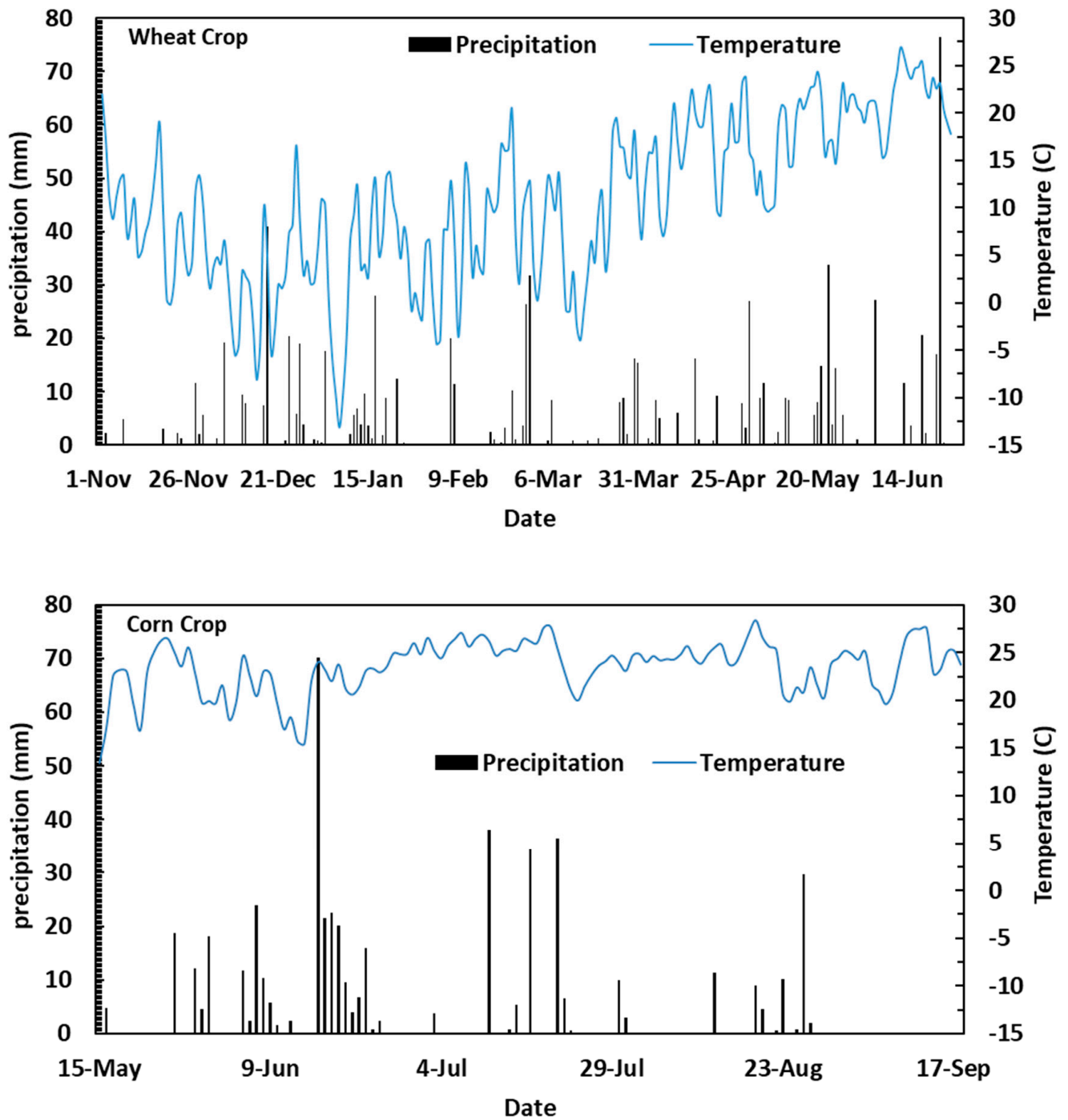


Figure 1. Daily precipitation and mean air temperature during the wheat growing season in 2016–2017 and corn growing season in 2019.

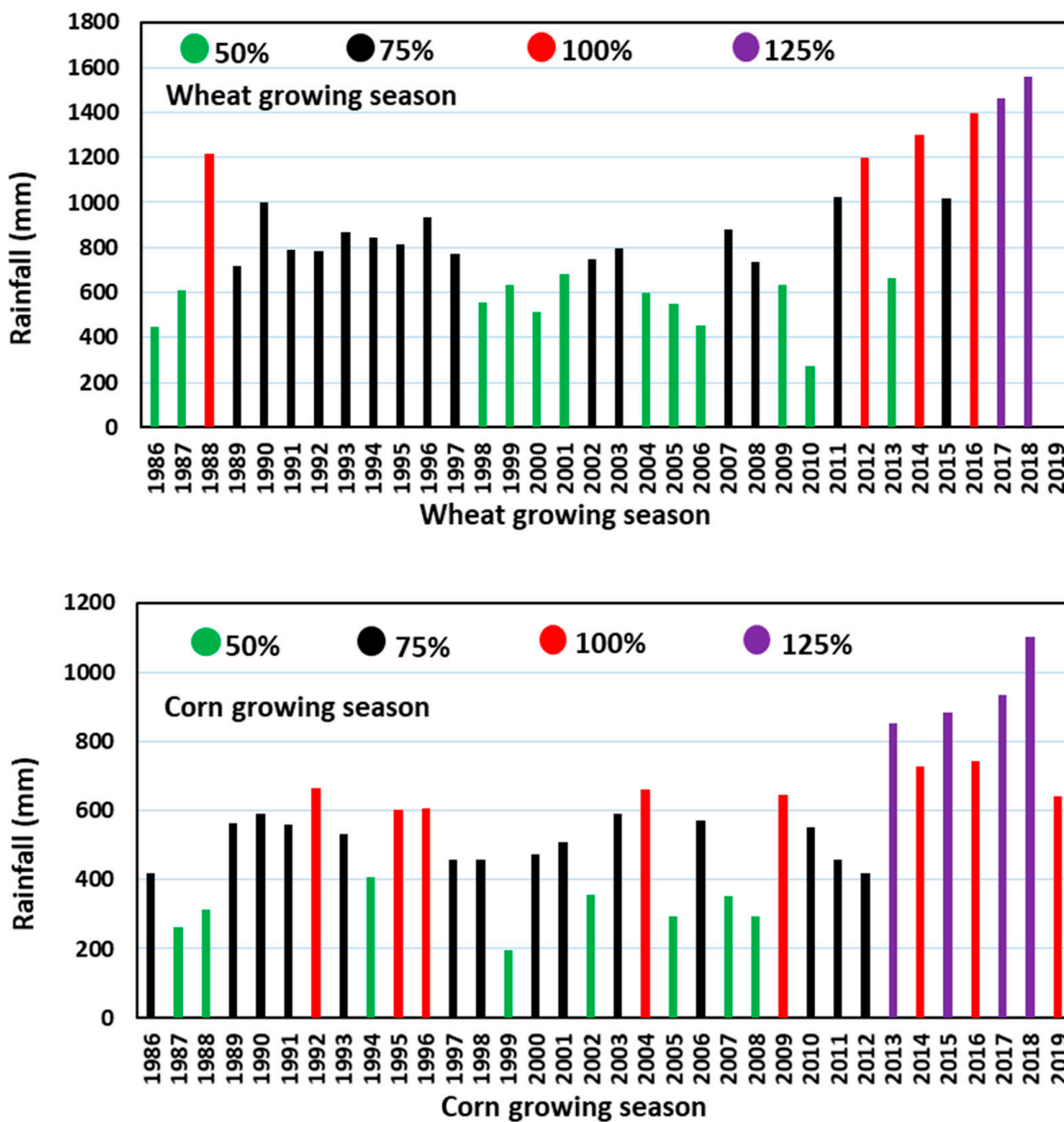


Figure 2. For the wheat growing season, 100% is the 2016–2017 season (red color category). For the corn growing season, 100% is the 2019 season (red color category). When multiplying the wheat/corn growing seasons by 50%, the results are shown by the green color category. For example, the growing seasons of 2001 and 1988 for wheat and corn, respectively. When multiplying the wheat/corn growing seasons by 75%, the results are denoted by the black color category. For example, the growing seasons of 1990 and 2000 for wheat and corn, respectively. When multiplying the wheat/corn growing seasons by 125%, the results are denoted by the purple color category. For example, the growing seasons of 2018 and 2013 for wheat and corn, respectively.

2.3. RZWQM2 Calibration

The main points of the model calibration processes are briefly described here. The RZWQM2 model requires a huge base of input information. This input is divided into two parts, i.e., daily weather data and soil-crop information. The daily weather data (solar radiation, maximum and minimum temperature, wind speed, relative humidity, and rainfall) were used as input data for all model scenarios before operating the model. Likewise, the soil profile depths and horizons, drainage information, planting and harvesting dates and methods, planting density and depth, row spacing, and irrigation and fertilizer application

method and rates were specified before using the model. Additional information such as the field area, elevation, latitude, slope, crop and surface albedos, residue mass, and age were also specified [47]. The soil profile was subdivided into ten layers. The depths of the model layers were 0–10, 10–20, 20–30, 30–40, 40–50, 50–60, 60–70, 70–80, 80–90, and 90–150 cm. Each simulation started three months ahead of planting to initialize the soil water based on the precipitation [30]. Soil mineral nitrogen was initialized using data from the first measurement campaign and is presented with other soil chemical characteristics in Table 2.

The model was calibrated for the wheat growing season using the experimental data from the N treatment of 130 kg N ha⁻¹ under the measured rainfall scenario of 100% rainfall as the model has a better response to the high nitrogen application rate than to a low nitrogen application rate [25]. The calibration process started with the soil moisture dynamics, then the N component, and finally the plant development components using the iterative calibration approach to have a satisfactory match between field-measured and model-simulated values of soil water dynamics, crop growth, mineral N, and crop evapotranspiration [27,48].

Because the physical and hydraulic properties (soil texture, dry bulk density, soil hydraulic conductivity, and soil water retention curve) of soil are very important model inputs, these properties were measured at several depths. The measured hydraulic property inputs (bulk density, saturated hydraulic conductivity, and water content at 0.10, 0.33, and 15 bar) were manually and iteratively modified within one standard error of measured values to achieve satisfactory correspondence between the field measurements and model simulations for the water content (Table 1). Soil properties were calibrated layer-by-layer (starting from the surface layer) until the best simulated soil water content was obtained for each layer.

During the calibration of the soil nutrient module, data for the first chemical measurement were used for model initialization (Table 2). The initial values of the slow, medium, and fast soil humus pools, i.e., fast and slow soil residue pools, and the three microbial pools, i.e., aerobic heterotrophs, autotrophs, and anaerobic heterotrophs, were set up. Field-measured values of soil organic-matter content at each layer were used to estimate the initial microorganism pools based upon the partitioning factors [1,6,49,50]. The model developers recommended partitioning the soil organic carbon at each layer between the fast/intermediate soil humus pools and slow soil humus pool, with 5–40% for the fast pools and 60–95% for the stable pool [51]. In our particular case, after many trials and errors with different initial partitions of soil-organic-carbon among pools, the best correspondence between field measurements and model-simulations of soil and crop nitrogen and crop growth was achieved when the differences between all pools were minimized. To obtain a stabilized fraction of the organic-matter pools and microorganism pools, a ten-year simulation was performed.

For the generic crop growth module, the planted cultivar (990003 WINTER-US) was used and its specific development parameters were adjusted to ensure a proper wheat yield, leaf area index, and above ground biomass simulations (Table 3) [52]. This adjustment was performed through successive runs of the model for the high N treatment. As the calibration of crop growth and development parameters is critical for the water and nutrient balance [28], the crop parameters were iteratively calibrated to have a satisfactory match between field-measured and model-simulated values of crop growth, soil water dynamics, and crop evapotranspiration.

Table 3. Calibrated crop parameters for wheat and corn crop.

Wheat cultivar Crop parameters of chosen wheat cultivar (990003 WINTER-US)	Calibrated
P1V: Days at an optimum vernalizing temperature required to complete vernalization	38
P1D: Percentage reduction in development when the photoperiod is 10 h less than the threshold (P1DT = 20 h) relative to that threshold	98
P5: Grain filling (excluding lag) phase duration (days)	500
G1: Kernel number per unit canopy weight at anthesis (#/g)	26
G2: Standard kernel size under optimum conditions (mg)	27
G3: Standard, non-stressed dry weight (total, including grain) of a single tiller at maturity (g)	1.5
PHINT: Interval between successive leaf tip appearances (days)	100
Corn cultivar Crop parameters of chosen corn cultivar (PC0004 2700-2750 GDD)	Calibrated
P1: Thermal time from seeding emergence to the end of the juvenile phase (days above 8 °C base temperature)	240
P2: Delay in development (days/h) for each hour that daylength is above 12.5 h (0–1)	0.75
P5: Thermal time from silking to physiological maturity (days above 8 °C base temperature)	850
G2: Maximum possible number of kernels per plant	800
G3: Kernel filling rate during the linear grain filling stage and under optimum conditions (mg/day)	8.5
PHINT: Phyllochron interval, i.e., the interval in thermal time (days) between successive leaf tip appearances	49
Maximum plant height at maturity (cm)	250
Plant biomass at half of maximum height (g)	200

For the corn growing season, the model was calibrated using the data of the corn growing season from 2016, which were presented by [18]. The corn growing season of 2019 was simulated by using calibrated soil, crop, and nutrient parameters of the corn growing season in 2016.

After the separate calibration of each model component, the simulated results of all components were checked and, if necessary, calibration was repeated until accurate model simulations were obtained. The calibrated model was used for simulating the effects of different nitrogen rates on soil water dynamics, crop evapotranspiration, and wheat and corn growth under four rainfall scenarios with 100%, 125%, 75%, and 50% of the rainfall. These scenarios were created in the RZWQM2 by multiplying the actual rainfall of each growing season (wheat and corn) by 1.25, 1.00, 0.75, and 0.50, respectively.

Three statistical criteria were used for the comparison between the simulations and measurements: (i) the root mean squared error (*RMSE*); (ii) mean bias error (*MBE*); and (iii) normalized root mean square errors (*NRMSE*). Low values of the *RMSE*, *NRMSE*, and *MBE* were the criteria for accepting the model performance and simulation accuracy [23,53].

$$RMSE = \sqrt{\frac{1}{n} \sum_{i=1}^n (P_i - O_i)^2} \quad (8)$$

$$MBE = \frac{1}{n} \sum (P_i - O_i) \quad (9)$$

$$NRMSE = \frac{RMSE}{O_{avg}} \quad (10)$$

where O_i is the measured value, P_i is the simulated value, O_{avg} is the mean of the measured values, and n is the number of data pairs. The RMSE reflects a magnitude of the mean difference between measured and simulated results. The MBE indicates a systematic positive or negative bias in the model simulations. The NRMSE indicates the suitability of the model. A perfect match between experimental and simulation results would yield an NRMSE = 0 [54].

3. Results and Discussions

RZWQM2 has been chosen to simulate the effect of applied N fertilizer on soil water dynamics and ETc under different rainfall conditions because it has been shown to accurately represent soil water dynamics and crop ETc with a high temporal resolution [19,24,25,29]. The RZWQM2 model reflected the impact of nitrogen application rates on the daily soil water dynamics, crop evapotranspiration, and crop growth under different N rates. When the first application (35 kg N ha^{-1}) was added to the wheat plots of the high N and low N treatments on day 132 of the growing season, the model simulations were different from the simulations of the zero N treatment. Also, when the second application was added on day 148 of the growing season, the high N simulation results differed from the low N simulations as 95 kg N ha^{-1} was applied with the high N treatment, whereas only 35 kg N ha^{-1} was applied with the low N treatment.

The soil water contents at different soil profile depths were simulated under different N rates and rainfall scenarios. Under the 100% rainfall scenario and during both growing seasons, SWC was simulated with RMSE and MBE between 0.00 and $0.09 \text{ cm}^3/\text{cm}^3$ for all soil depths and N rates. The NRMSE was less than 0.2 for the same soil depths and N rates during the wheat growing season. While, during the corn growing season, SWC was simulated with higher values of NRMSE for all soil depths and N rates (Figures 3 and 4). Generally, the RMSE, MBE, and NRMSE values were decreased with an increasing depth. These results are statistically comparable to those found in other studies with [23] different N treatments and [20] the use of two generic modules of the RZWQM.

In the 100% and 125% rainfall scenarios, the highest SWC was simulated under the high N rate scenario at all soil depths, while the zero N rate presented the lowest SWC which may be due to the effect of high soil evaporation under the zero N rate during both crop growing seasons (Figures 3–5). The differences between simulated SWC under different N rates decreased with an increasing soil depth. On the other hand, under the 75% and 50% rainfall scenarios, no difference in the effect of N rates on the SWC at all soil depths was observed. This is probably due to the soil water availability and its movement, as well as the water stress (Figure 5). As seen in Figure 5, all N rates overlapped for the 50% and 75% rainfall scenarios.

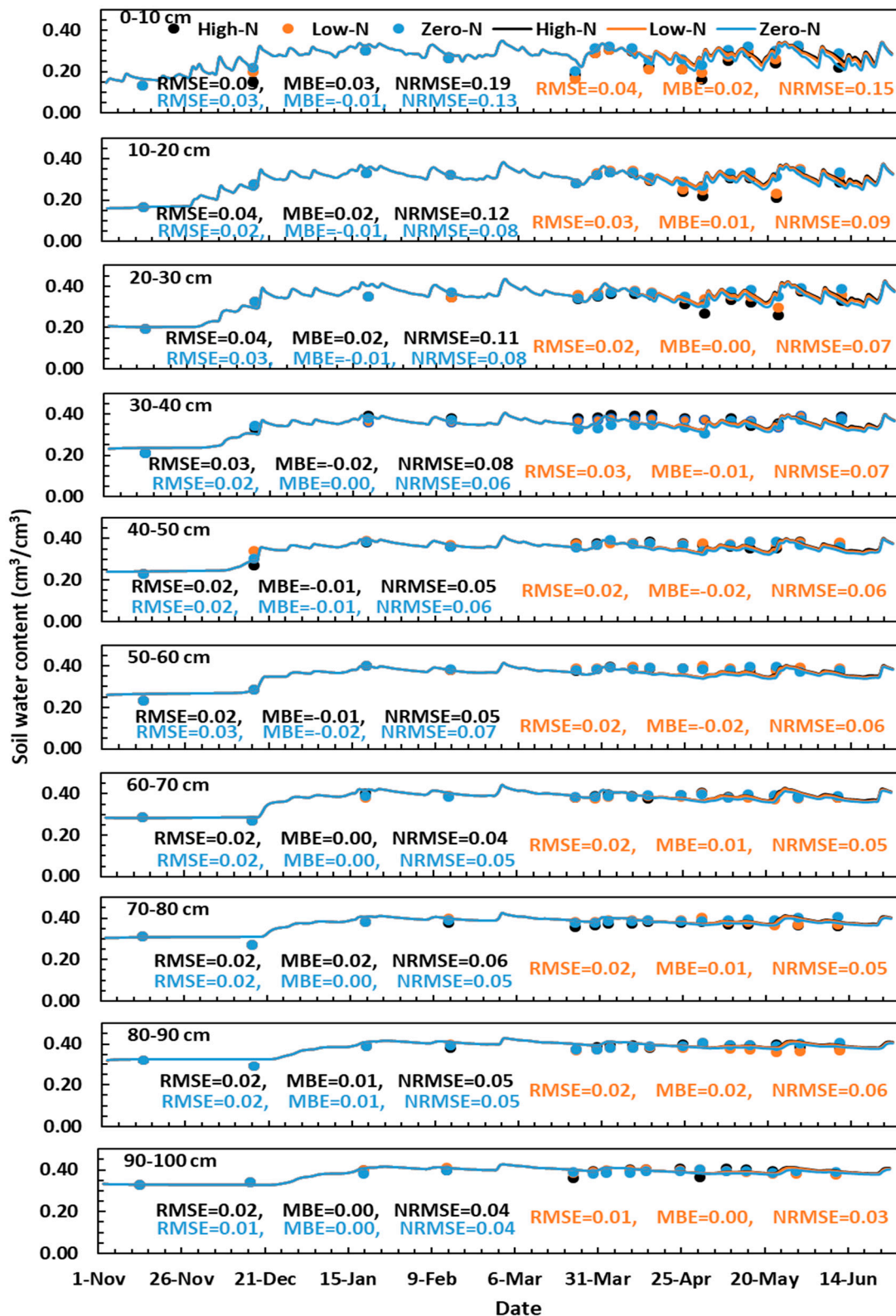


Figure 3. Model-simulated vs. field-measured soil water contents with time in different soil layers for the high N, low N, and zero N rates during the wheat growing season under 100% rainfall.

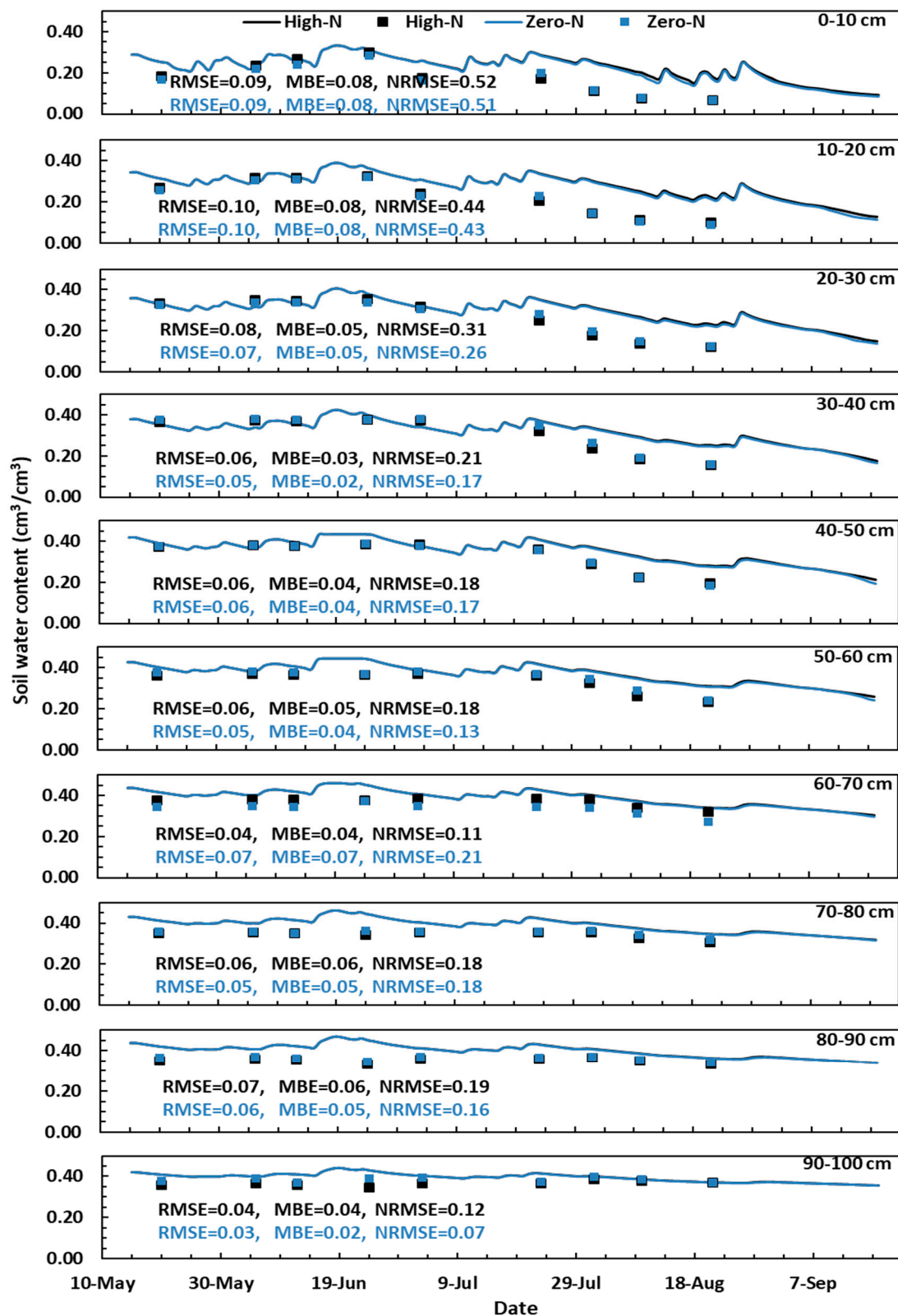


Figure 4. Model-simulated vs. field-measured soil water content with time in different soil layers for the high N and zero N rates during the corn growing season under 100% rainfall.

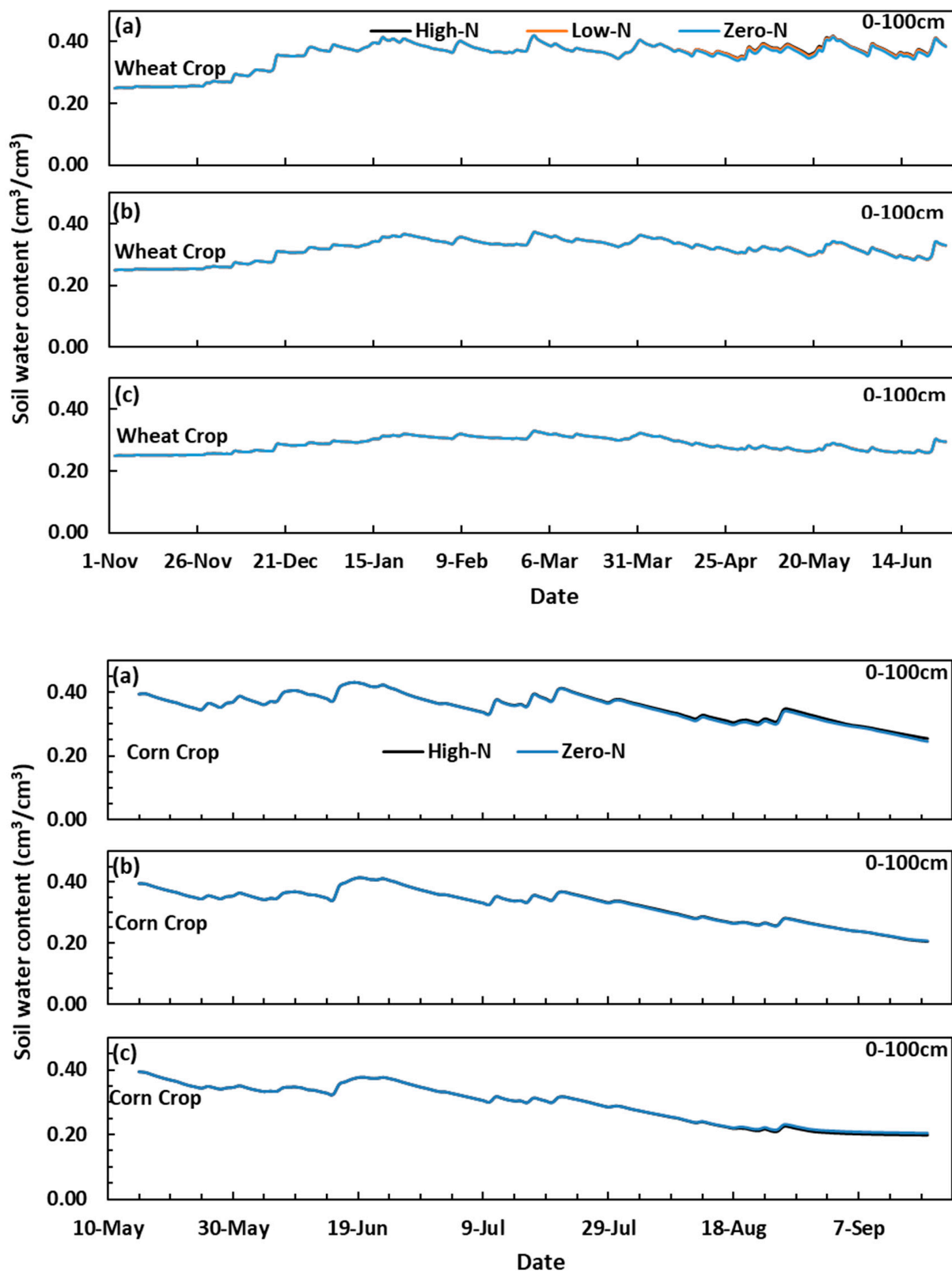


Figure 5. Model-simulated soil water content with time for a 0–100 cm soil depth, during the wheat and corn growing seasons under the (a) 125%, (b) 75%, and (c) 50% rainfall scenarios.

The measured soil water flux for the days with measurements of SWC and simulated SWF across the 90 cm plane of the root zone for all N rates and under different rainfall scenarios are presented in Figure 6. Under the 100% rainfall scenario and during the wheat growing season, the model produced reasonable results of SWF through the bottom boundary with RMSE of 1.06, 0.96, and 1.08 mm/day for the high N, low N and zero N rates, respectively; however, the RMSE values were slightly higher during the corn growing season (Figure 6), which is within the range stated in [55]. Under the 100% and 125% rainfall scenarios, the high N rate yielded the highest SWF out of the root zone, while the lowest SWF out of the root zone occurred with the zero N rate during both growing seasons. This simulation result was probably observed due to the fact that the high N rate presented high crop cover, which reduced the soil evaporation and increased the soil water flux out of the root zone (Figure 6a,b); however, all the N rates presented similar SWF under the 75% and 50% rainfall scenarios for both growing seasons (Figure 6c,d). When the amount of rainfall was increased from 100% to 125%, the SWC was unchanged at all soil depths due to the limitation of the soil water holding capacity. The SWF out of the root zone was clearly increased with increasing the amount of rainfall; however, SWC and SWF were decreased with decreasing rainfall to 75% and 50%.

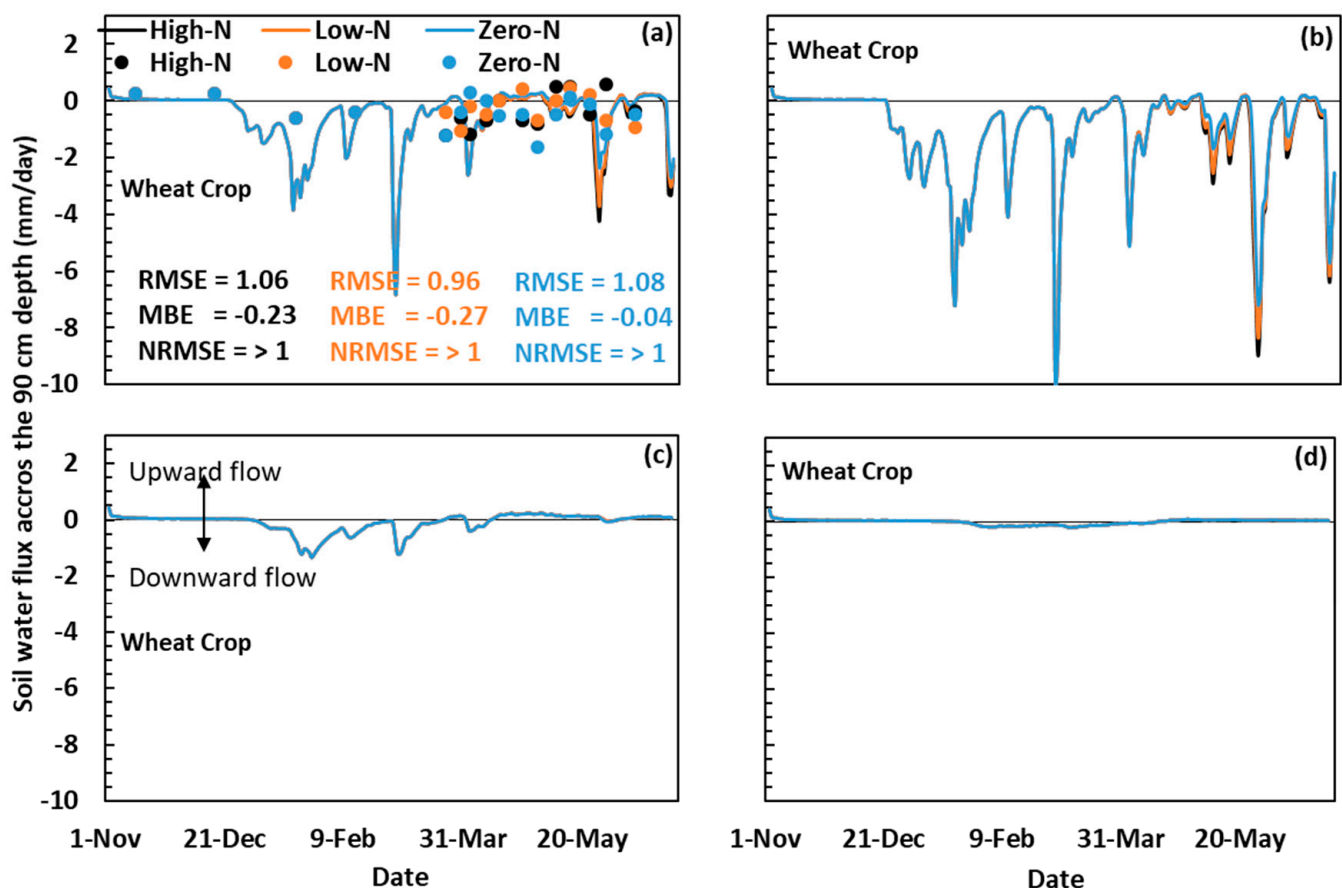


Figure 6. Cont.

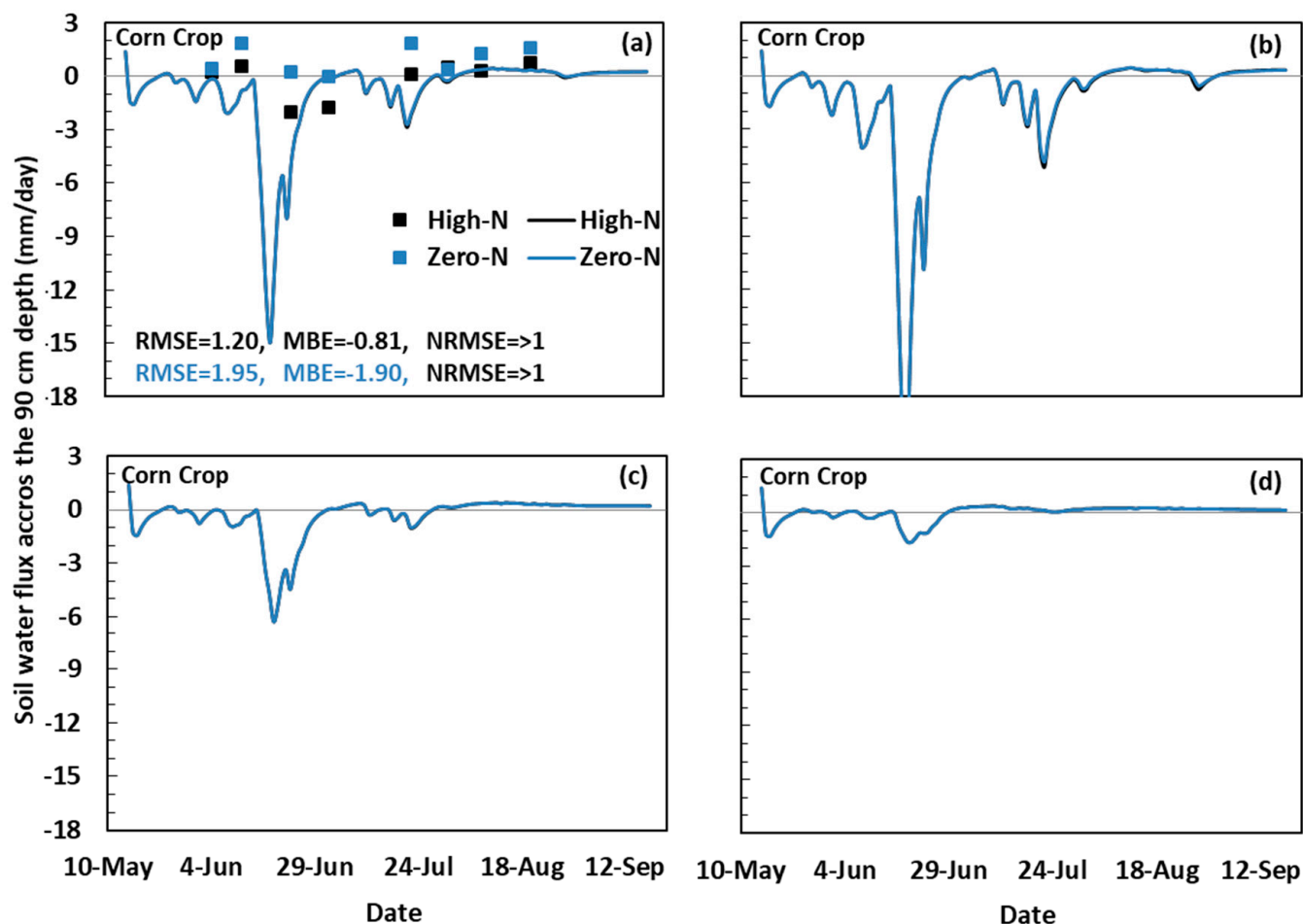


Figure 6. Soil water flux across the 90 cm plane of the root zone for the wheat and corn growing seasons when under the (a) 100%, (b) 125%, (c) 75%, and (d) 50% rainfall scenarios.

As the E_{Tc} is partitioned between crop transpiration and soil evaporation [56], the leaf area index is one of the most critical crop growth parameters. The simulated LAI directly impacts the simulated evapotranspiration and influences the soil water dynamics. Figure 7a shows the RMSE values under the 100% rainfall scenario which were 0.42, 0.32, and 0.53 for the high N, low N and zero N conditions, respectively, for the wheat growing season. LAI was simulated for the corn growing season with RMSE of 0.54 and 0.44 for the high N and zero N conditions, respectively, which is lower than RMSE values reported by [24].

During both growing seasons, the high N rate showed higher LAI values than the other N rates under the 100%, 125%, and 75% rainfall scenarios (Figure 7a–c); however, under the 50% rainfall scenario, there was a slight impact of the N rate on crop growth, and the LAI values were almost identical for all N rates when water stress appeared under the drought conditions (Figure 7d). The 75% rainfall scenario produced higher LAI values for all N rates than the 100% and 125% rainfall scenarios; however, the 50% rainfall scenario presented higher LAI values for the zero N rate than the other rainfall scenarios. The reason behind these results could be the influence of the SWF, which was higher under the 100% and 125% rainfall scenarios than the others. When the SWF out of the root zone increases, the lost mineral N out of the root zone increases as well, whereas the N uptake decreases, which affects the crop growth (Table 4).

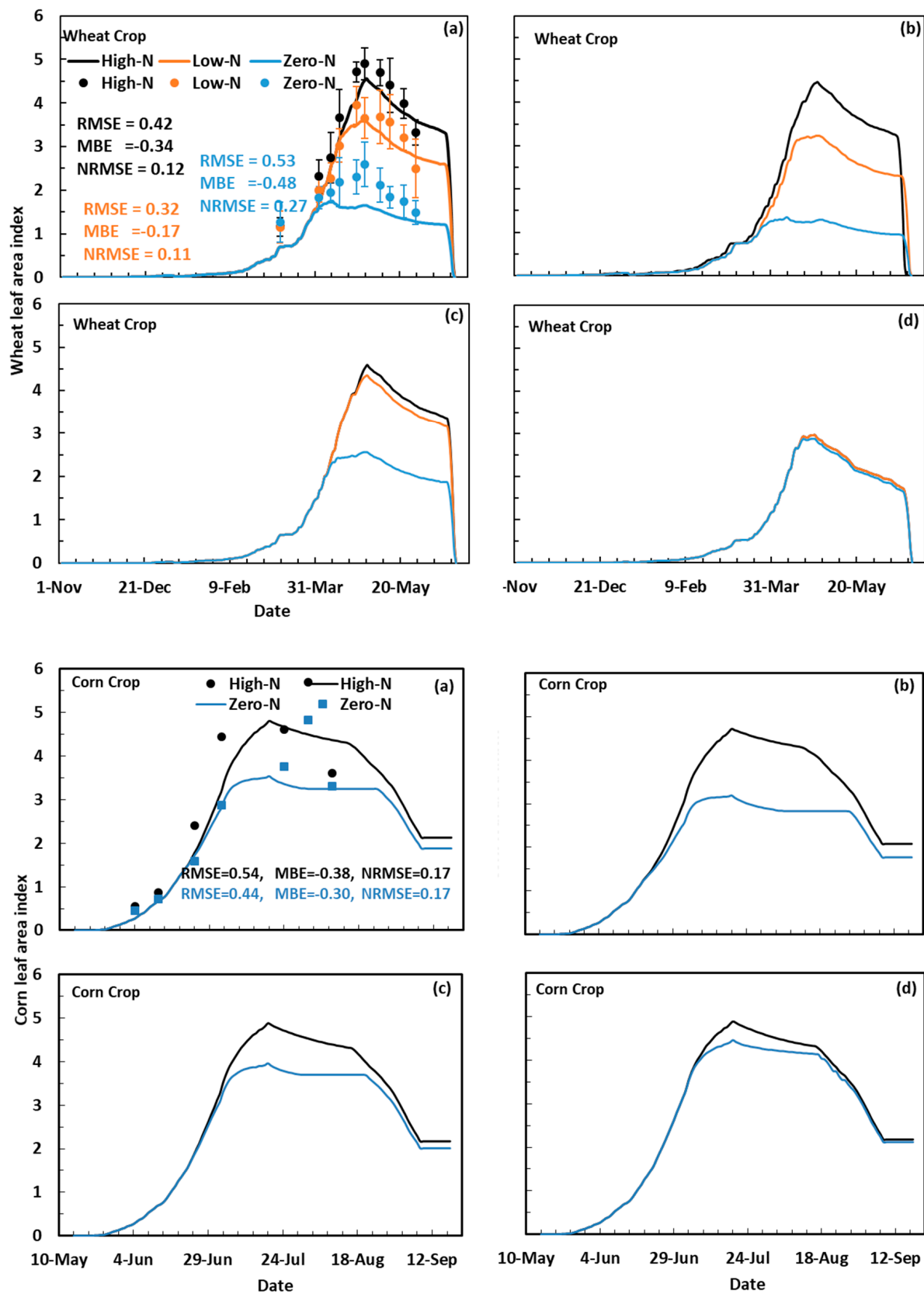


Figure 7. Leaf area index for the wheat and corn growing seasons under the: (a) 100%, (b) 125%, (c) 75% and (d) 50% rainfall scenarios.

Table 4. Simulated total water uptake (mm) and N uptake (kg/ha) from the soil profiles for wheat and corn over the growing seasons.

		Water Uptake (mm)			
		50%	75%	100%	125%
Wheat	High N	186	266	267	267
	Low N	186	265	261	254
	Zero N	184	246	238	210
Corn	High N	274	322	324	323
	Zero N	268	314	324	315
		Nitrogen Uptake (kg/ha)			
		50%	75%	100%	125%
Wheat	High N	164	232	231	231
	Low N	164	218	188	188
	Zero N	160	158	122	122
Corn	High N	291	316	315	313
	Zero N	266	296	283	269

Table 4 shows the total simulated N uptake for wheat and corn growing seasons. The amount of soil nitrogen in the soil profile is very affected by the received rainfall amount because it can be leached out of the soil profile under high rainfall amounts. For the high N treatment, no substantial differences in the N uptake were observed among all rainfall scenarios except the 50% scenario during both growing seasons; however, under the impact of the low N treatment, the 75% scenario presented higher N uptake than the 100% and 125% scenarios by 0.14 and higher than the 50% scenario by 0.25. The reason behind this is the received rainfall amount, where under the impact of the 100% and 125% scenarios, the soil nitrogen leached out of the soil profile due to the high rainfall amount, while, under the 75% scenario, the rainfall was not excessive and the nitrogen did not leach out of the soil profile (Figure 8). The N uptake of the 50% scenario was lower than under all other rainfall scenarios for the high N and low N treatments; however, the zero N treatment presented lower N uptake under the 100% and 125% scenarios due to the impact of excessive rainfall and the leaching process. As such, it is demonstrated that the N uptake is conversely affected by increasing the amount of excessive water.

Table 4 shows the water uptake under different levels of applied nitrogen and received rainfall. The high N treatment presented almost similar values of water uptake for all rainfall scenarios except the 50% scenario. Due to the water deficiency, that scenario showed a water uptake lower by about 0.3 and 0.15 for wheat and corn growing seasons, respectively, than the other scenarios; however, the 75% scenario gave higher water uptake than the other scenarios. Although there was abundant water under the 100% and 125% scenarios, they showed lower water uptake than the 75% scenario during the wheat growing season due to the impact of nitrogen leaching, which affects the plant growth and then the water uptake. Under the impact of the zero N treatment, the 75% scenario presented the highest water uptake for the wheat growing season; however, for the corn growing season, the 100% scenario yielded the highest water uptake. As such, the corn crop consumed more water if there was abundant water in the soil.

Water and nitrogen use efficiency were simulated for the interaction between the rainfall amount and nitrogen rate (Table 5). For the wheat crop, the 50% rainfall scenario yielded the highest WUE, while the WUE was decreased with increasing the rainfall amount. Also, the WUE decreased with a decreasing nitrogen application rate, and the reduction was between 0.02 to 0.4 kg/m³. For the corn crop, the rainfall scenario of 75% and 100% yielded higher WUE than the other scenarios. The WUE of the corn was also decreased for a lower nitrogen application rate. These results were in agreement with the findings of [57,58].

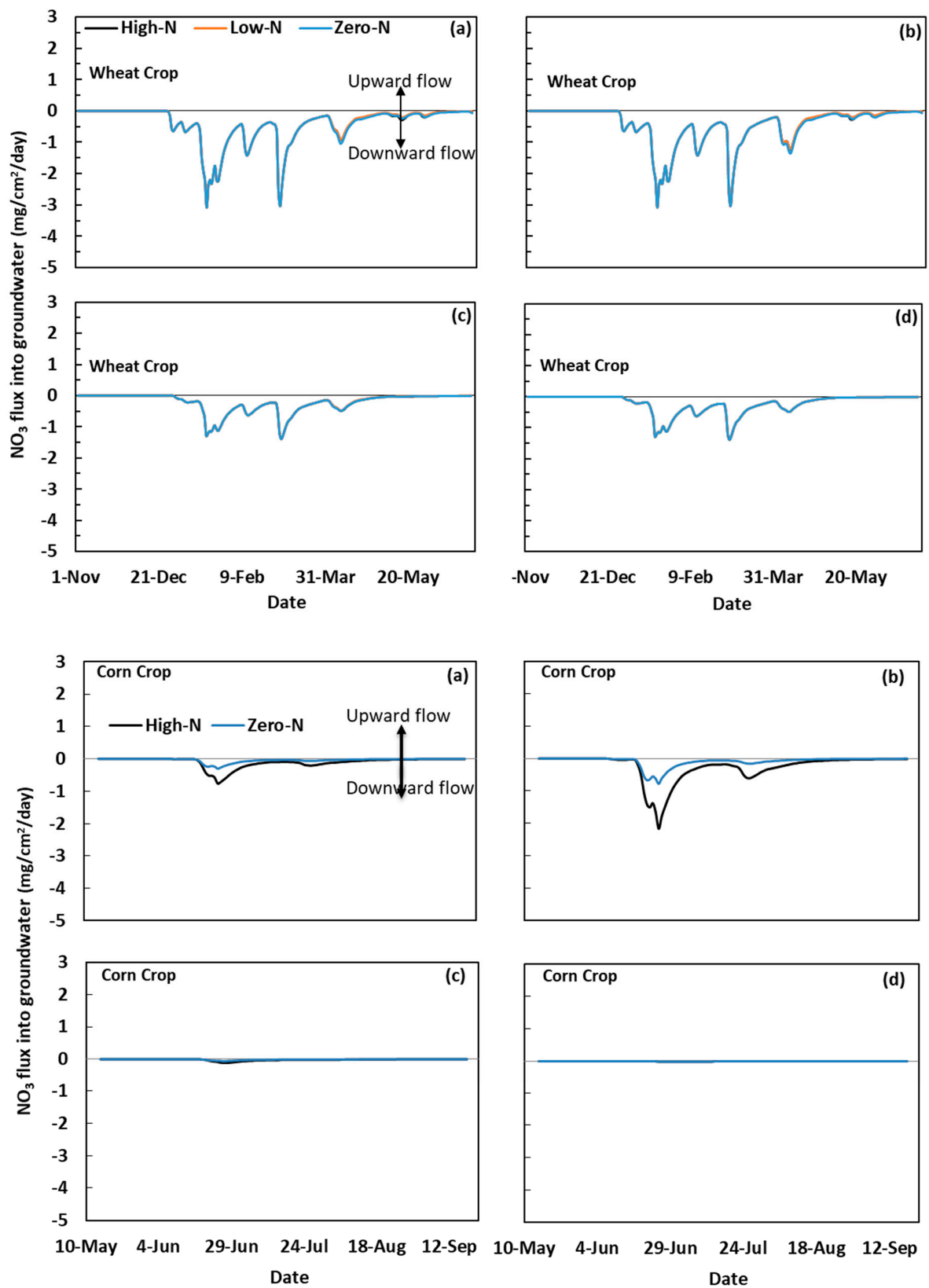


Figure 8. Simulated NO₃ flux into groundwater for the wheat and corn growing seasons under the: (a) 100%, (b) 125%, (c) 75%, and (d) 50% rainfall scenarios.

Table 5. Simulated water use efficiency (kg/m³) and nitrogen use efficiency for wheat and corn crop.

		Water Use Efficiency			
		50%	75%	100%	125%
Wheat	High N	2.1	1.4	1.3	1.2
	Low N	1.8	1.1	1.0	0.9
	Zero N	1.3	0.7	0.6	0.5
Corn	High N	2.1	2.4	2.4	2.3
	Zero N	1.9	2.2	2.1	2.0
		Nitrogen Use Efficiency			
		50%	75%	100%	125%
Wheat	High N	22.3	26.3	28.4	28.7
	Low N	25.6	29.8	32.0	32.2
Corn	High N	5.6	6.7	7.3	7.4

The simulation results of NUE are also presented in Table 5. The rainfall scenario of 125% produced the highest NUE than the other rainfall scenarios for both crops. The low N treatment yielded a better result of NUE than the high N treatment for all rainfall scenarios, which means that there probably was an excess of applied nitrogen in the high N treatment that may be leached out of the root zone. This finding was comparable with the results of [59].

The daily average actual crop evapotranspiration was calculated over roughly 7 day periods using the soil water balance method (SWB). During the wheat growing season, the model resulted in satisfactory values of RMSE, MBE, and NRMSE for all N rates under the 100% rainfall scenario (Figure 9). With RMSE values of 1.23, 1.43, and 1.60 mm/day, the ET_c was simulated for high N, low N, and zero N conditions, respectively. Statistically, ET simulations for all N rates were comparable to the findings shown in [24,25]. A zero N rate produced the highest simulated ET_c for the period of 156–215 days after sowing; however, it produced the lowest simulated ET_c for the rest of the wheat growing season due to the influence of simulated LAI (Figure 9).

During the corn growing season, the model underestimated the ET_c, especially during the development stage with a MBE of −0.74 and −0.60 mm/day for the high N and zero N conditions, respectively. The ET_c was simulated for high N and zero N with RMSE values of 1.94 and 1.59 mm/day, respectively. Similarly, regarding the ET_c of wheat, the zero N rate produced higher simulated ET_c than the high N for the corn.

Figure 10a,b show a comparison of simulated cumulative actual crop transpiration, actual soil evaporation, and actual crop evapotranspiration among all N rates for wheat under 100% and 125% rainfall scenarios. As expected, the highest cumulative simulated crop transpiration was presented under high N rates, while a zero N rate presented lower simulated crop transpiration than the other N rates because the simulated LAI of the zero N rates did not reach values of 3. Simulated soil evaporation under a zero N rate was higher than for the other N rates, particularly under the 125% rainfall scenario due to the soil's ability to evaporate all the abundant soil water. This might explain why the cumulative ET_c was higher for zero N than the other rates.

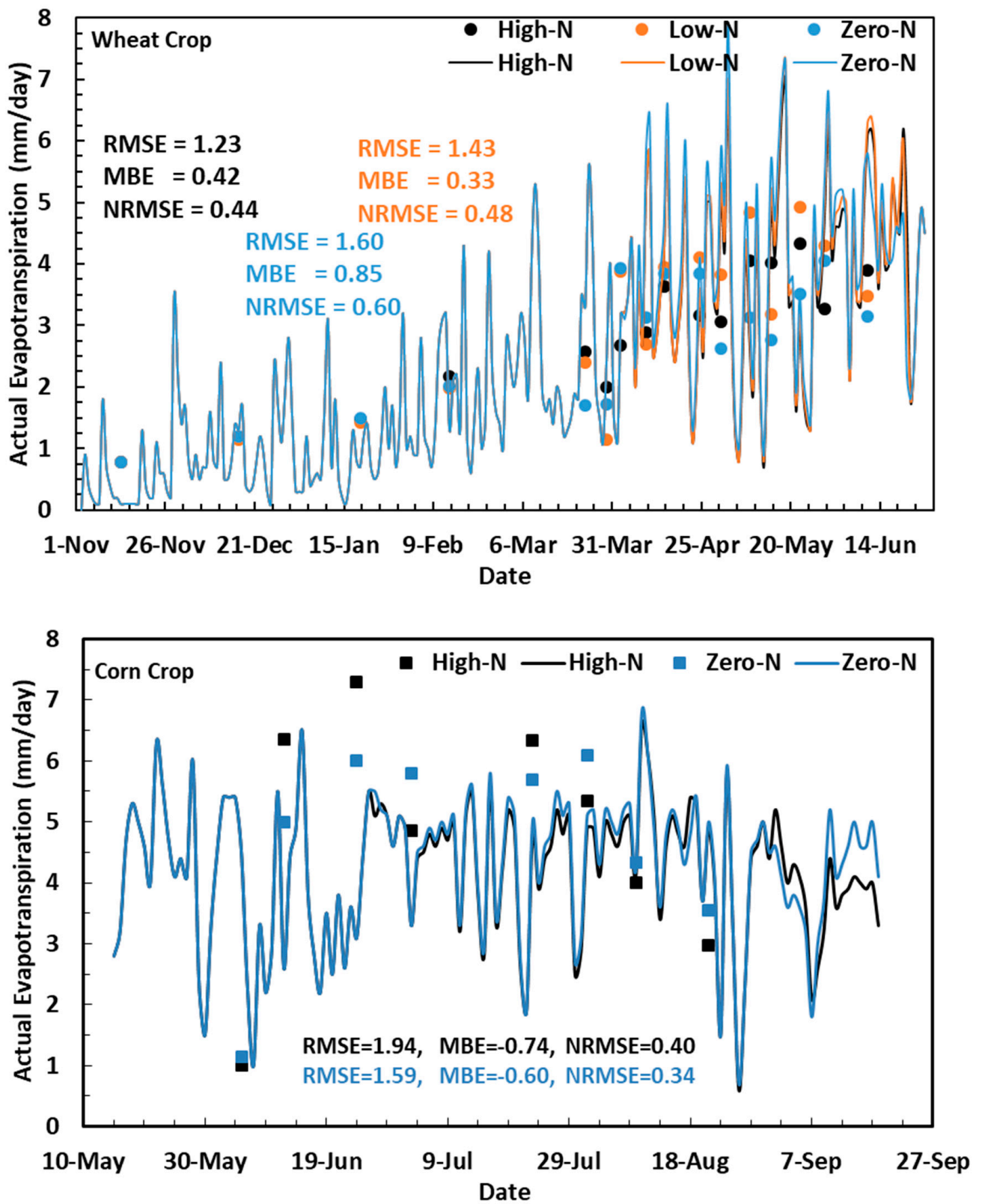


Figure 9. Simulated vs. field-measured actual crop evapotranspiration for the wheat and corn growing seasons under the 100% rainfall scenario.

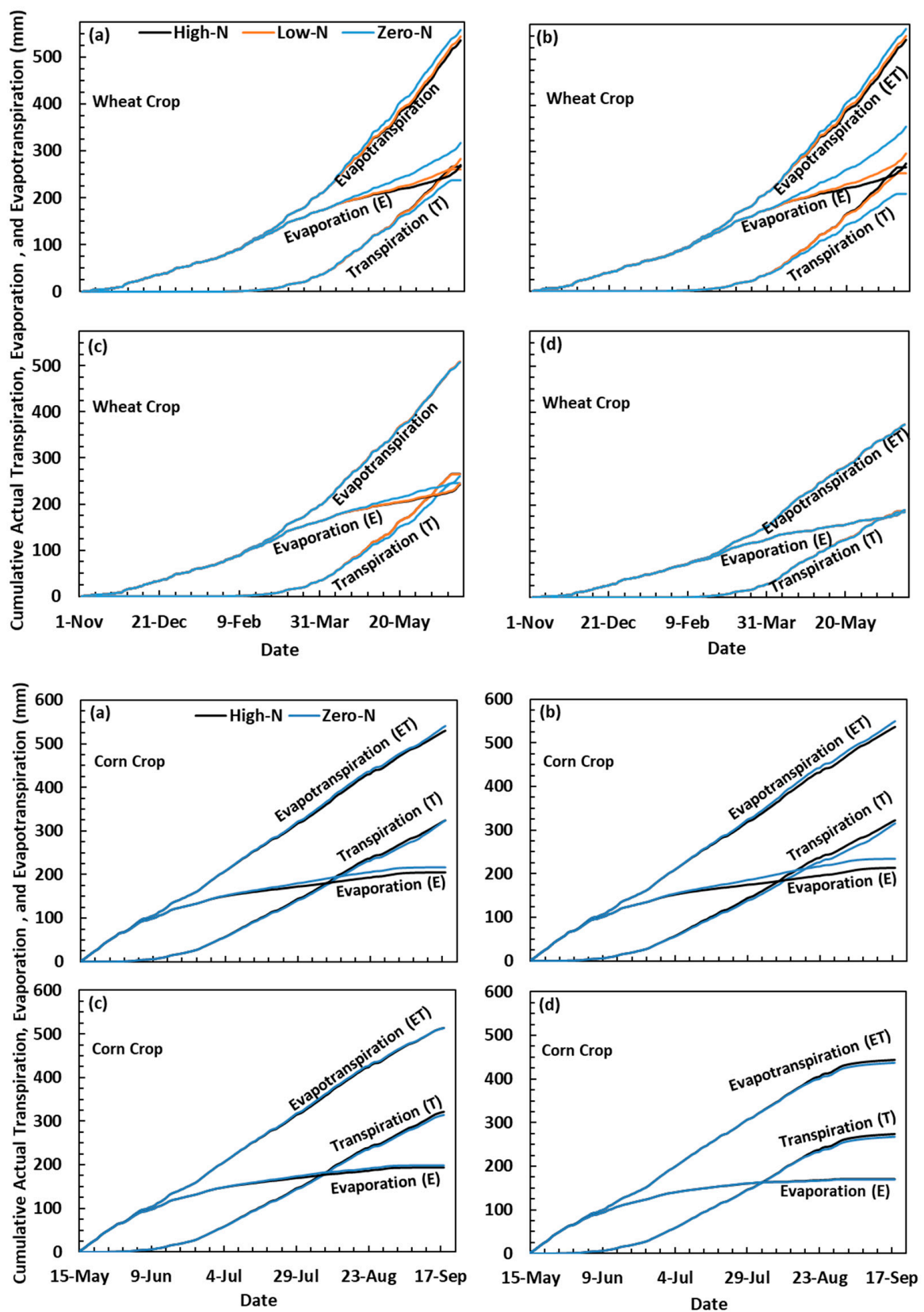


Figure 10. Cumulative actual transpiration, evaporation, and evapotranspiration (mm) for the wheat and corn growing seasons under the: (a) 100%, (b) 125%, (c) 75% and (d) 50% rainfall scenarios.

Figure 10c shows simulated crop transpiration, soil evaporation, and evapotranspiration under 75% rainfall for the wheat crop. Under the 75% rainfall scenario, the high N and low N rates showed similar values of crop transpiration, as well as similar values of soil evaporation; however, the crop transpiration and soil evaporation values of the zero N rates were differentiated from the other N rates. The ETC values were similar for all N rates. From the results of the 100%, 125%, and 75% scenarios, we conclude that under high rainfall amounts, the soil evaporated higher amounts of water, which made the ETC of the low crop cover higher than ETC of the high crop cover. In other words, the increase in simulated soil evaporation was higher than the increase of the simulated crop transpiration which yielded a higher simulated ETC for the zero N rate than for the other N rates.

Figure 10d shows crop transpiration, soil evaporation, and evapotranspiration under the 50% rainfall scenario. In this scenario, all N rates produced similar values for crop transpiration, soil evaporation, and evapotranspiration due to drought conditions, which limited the LAI to less than three for all N rates.

Regarding the corn crop, simulated cumulative actual crop transpiration, actual soil evaporation, and actual crop evapotranspiration under different N rates presented similar trends to the wheat crop; however, the corn growing season presented smaller differences than the wheat growing season among N rates as the simulated corn LAI exceeded three for both N rates at the beginning of the growing season. When the simulated LAI became three or more, the model behaved similarly for all N rates with regards to simulating ETC and its components. As mentioned by [33,39,40], most crop leaves contribute to crop transpiration when the LAI is less than three; however, the transpiration does not reach the maximum amount until the LAI becomes three or more. This confirms the above description that the leaf area index becomes a non-limiting factor for evapotranspiration when it has a value of three or larger, and crops with a LAI of three or larger will have the same evapotranspiration rate if soil water is not a limiting factor [41,60,61].

4. Conclusions

The RZWQM2 model was used in this work to quantify the effects of various N application rates on the soil water dynamics and ETC behaviors of rainfed wheat and corn under different rainfall scenarios. The results indicate that the model performed satisfactorily in simulating the impacts of the N rate and rainfall on the soil and crop water dynamics. The N application rate showed a noticeable influence on the simulated soil-crop water dynamics. Furthermore, this influence was differentiated based on the received rainfall amounts. Simulated crop transpiration increased with an increasing N rate, whereas soil evaporation increased with a decreasing N rate. Nitrogen application rates appreciably manipulated the crop evapotranspiration and soil water dynamics under high rainfall amounts; however, under low rainfall amount, soil water dynamics and crop evapotranspiration were not affected by N application rates. N uptake was conversely affected by excessive rainfall amounts.

The results of this study not only provide indications for using the RZWQM2 as an agricultural management tool but also show the applicability of the RZWQM2 for improving the scientific understanding of the interaction between N application rates and water dynamics in the field. Similar testing across diverse crop, soil, and rainfall conditions could be a critical need in the future to build a better understanding of the climatic impact on WUE and NUE. Also, the use of weighing lysimeters under similar test conditions could be a good method to improve the understanding of the interaction between N application rate and ETC behavior as, by using the lysimeters, the applied and evaporated water can be accurately measured over an entire crop growth season.

Author Contributions: Writing—original draft preparation, S.S.S.; writing—review and editing, S.S.S., O.W. and D.D. supervision, O.W.; project administration, O.W.; methodology, S.S.S. and D.D.; software and analysis, S.S.S. All authors have read and agreed to the published version of the manuscript.

Funding: This research received no external funding.

Institutional Review Board Statement: Not applicable.

Informed Consent Statement: Not applicable.

Data Availability Statement: Not applicable.

Conflicts of Interest: The authors declare no conflict of interest.

References

- Ahuja, L.; Ma, L. *Parameterization of Agricultural System Models: Current Approaches and Future Needs*; Agricultural System Models in Field Research and Technology Transfer; Lewis Publishers: Boca Raton, FL, USA, 2002.
- Ahuja, L.; Rojas, K.; Hanson, J.; Shaffer, M.; Ma, L. *Root Zone Water Quality Model: Modeling Management Effects on Water Quality and Crop Production*; Water Resources Publ., LLC: Highland Ranch, CO, USA, 2000; p. 372.
- Alves, I.; Maria, D.R.C. Evapotranspiration Estimation Performance of Root Zone Water Quality Model: Evaluation and Improvement. *Agric. Water Manag.* **2002**, *57*, 61–73. [[CrossRef](#)]
- Anapalli, S.S.; Ahuja, L.R.; Gowda, P.H.; Ma, L.; Marek, G.; Evett, S.R.; Howell, T.A. Simulation of Crop Evapotranspiration and Crop Coefficients with Data in Weighing Lysimeters. *Agric. Water Manag.* **2016**, *177*, 274–283. [[CrossRef](#)]
- Cameira, M.R.; Sousa, P.L.; Farahani, H.J.; Ahuja, L.R.; Pereira, L.S. Evaluation of the RZWQM for the Simulation of Water and Nitrate Movement in Level-Basin, Fertigated Maize. *J. Agric. Eng. Res.* **1998**, *69*, 331–341. [[CrossRef](#)]
- Cameira, M.; Fernando, R.; Ahuja, L.; Ma, L. Using RZWQM to Simulate the Fate of Nitrogen in Field Soil–Crop Environment in the Mediterranean Region. *Agric. Water Manag.* **2007**, *90*, 121–136. [[CrossRef](#)]
- Cameira, M.; Fernando, R.; Ahuja, L.; Pereira, L. Simulating the Fate of Water in Field Soil—Crop Environment. *J. Hydrol.* **2005**, *315*, 1–24. [[CrossRef](#)]
- Camillo, P.J.; Gurney, R.J. A Resistance Parameter for Bare-Soil Evaporation Models. *Soil Sci.* **1986**, *141*, 95–105. [[CrossRef](#)]
- Djaman, K.; Irmak, S. Actual Crop Evapotranspiration and Alfalfa-and Grass-Reference Crop Coefficients of Maize under Full and Limited Irrigation and Rainfed Conditions. *J. Irrig. Drain. Eng. ASCE* **2013**, 433–446. [[CrossRef](#)]
- Fang, Q.; Ma, L.; Yu, Q.; Malone, R.; Saseendran, S.; Ahuja, L. Modeling Nitrogen and Water Management Effects in a Wheat-Maize Double-Cropping System. *J. Environ. Qual.* **2008**, *37*, 2232–2242. [[CrossRef](#)]
- Farahani, H.; DeCoursey, D. Potential Evaporation and Transpiration Processes in the Soil-Residue-Canopy System. In *RZWQM, Modeling Management Effects on Water Quality and Crop Production*; Ahuja, L., Rojas, K., Hanson, J., Shaffer, M., Ma, M., Eds.; Water Resources Publications, LLC: Littleton, CO, USA, 2000; pp. 51–75.
- Farahani, H.; Ahuja, L. Evapotranspiration Modeling of Partial Canopy/Residue-Covered Fields. *Trans. ASAE* **1996**, *39*, 2051–2064. [[CrossRef](#)]
- Farahani, H.; Bausch, W. *Seasonal Application of Physical Evapotranspiration Models: Resistance Estimation*; ASAE: St Joseph, MI, USA, 1994; Volume 4, p. 2547.
- Farahani, H.J.; Buchleiter, G.W.; Ahuja, L.R.; Peterson, G.A.; Sherrod, L.A. Seasonal Evaluation of the Root Zone Water Quality Model in Colorado. *Agron. J.* **1999**, *91*, 212–219. [[CrossRef](#)]
- Frimpong, J.O.; Addy, M.Q.; Aye, E.O.; Amoatey, H.M.; Kutufam, J.T.; Quaye, B.; Sintim, J.O.; Asare, D.K. Field Assessment of Soil Water Storage and Actual Evapotranspiration of Rainfed Maize (*Zea mays* L.) Genotypes in a Coastal Savannah Environment. *Open J. Soil Sci.* **2012**, *2*, 213–222. [[CrossRef](#)]
- Gheysari, M.; Mirlatif, S.M.; Bannayan, M.; Homae, M.; Hoogenboom, G. Interaction of water and nitrogen on maize grown for silage. *Agric. Water Manag.* **2009**, *96*, 809–821. [[CrossRef](#)]
- Ham, J.; Heilman, J. Aerodynamic and Surface Resistances Affecting Energy Transport in a Sparse Crop. *Agric. For. Meteorol.* **1991**, *53*, 267–284. [[CrossRef](#)]
- Hanson, J. *Generic Crop Production Model for the Root Zone Water Quality Model. The Root Zone Water Quality Model*; Water Resource Publishing: Highland Ranch, CO, USA, 2000.
- Hanson, J.; Ahuja, L.; Shaffer, M.; Rojas, K.; DeCoursey, D.; Farahani, H.; Johnson, K.; Team, R.D. RZWQM: Simulating the Effects of Management on Water Quality and Crop Production. *Agric. Syst.* **1998**, *57*, 161–195. [[CrossRef](#)]
- Hanson, J.D.; Rojas, K.; Shaffer, M.J. Calibrating the Root Zone Water Quality Model. *Agron. J.* **1999**, *91*, 171–177. [[CrossRef](#)]
- Hu, C.; Saseendran, S.; Green, T.; Ma, L.; Li, X.; Ahuja, L. Evaluating Nitrogen and Water Management in a Double-Cropping System Using RZWQN. *Vadose Zone J.* **2006**, *5*, 493–505. [[CrossRef](#)]
- Irmak, S.; Istanbuluoglu, E.; Irmak, A. An Evaluation of Evapotranspiration Model Complexity against Performance in Comparison with Bowen Ratio Energy Balance Measurements. *Trans. ASABE* **2008**, *51*, 1295–1310. [[CrossRef](#)]
- Kang, S.; Gu, B.; Du, T.; Zhang, J. Crop Coefficient and Ratio of Transpiration to Evapotranspiration of Winter Wheat and Maize in a Semi-Humid Region. *Agric. Water Manag.* **2003**, *59*, 239–254. [[CrossRef](#)]
- Kristensen, K. Actual Evapotranspiration in Relation to Leaf Area. *Hydrol. Res.* **1974**, *5*, 173–182. [[CrossRef](#)]
- Kumar, A.; Kanwar, R.S.; Singh, P.; Ahuja, L.R. Evaluation of the Root Zone Water Quality Model for Predicting Water and No 3–N Movement in an Iowa Soil. *Soil Tillage Res.* **1999**, *50*, 223–236. [[CrossRef](#)]

26. Kunrath, T.R.; Lemaire, G.; Sadras, V.O.; Gastal, F. Water use efficiency in perennial forage species: Interactions between nitrogen nutrition and water deficit. *Field Crop. Res.* **2018**, *222*, 1–11. [[CrossRef](#)]
27. Li, Y.; Cui, S.; Zhang, Z.; Zhuang, K.; Wang, Z.; Zhang, Q. Determining effects of water and nitrogen input on maize (*Zea mays*) yield, water-and nitrogen-use efficiency: A global synthesis. *Sci. Rep.* **2020**, *10*, 9699. [[CrossRef](#)]
28. López-Bellido, L.; López-Bellido, R.J.; Redondo, R. Nitrogen Efficiency in Wheat Under Rainfed Mediterranean Conditions as Affected by Split Nitrogen Application. *Field Crop. Res.* **2005**, *94*, 86–97. [[CrossRef](#)]
29. Ma, L.; Ahuja, L.R.; Saseendran, S.A.; Malone, R.W.; Green, T.R.; Nolan, B.T.; Bartling, P.N.S.; Flerchinger, G.N.; Boote, K.J.; Hoogenboom, G. A Protocol for Parameterization and Calibration of RZWQM2 in Field Research. In *Methods of Introducing System Models into Agricultural Research*; Ahuja, L.R., Ma, L., Eds.; SSSA Book Series; American Society of Agronomy: Madison, WI, USA, 2011; pp. 1–64.
30. Ma, L.; Ahuja, L.R.; Ascough II, J.C.; Shaffer, M.J.; Rojas, K.W.; Malone, R.W.; Cameira, M.R. Integrating system modeling with field research in agriculture: Applications of the Root Zone Water Quality Model (RZWQM). *Adv. Agron.* **2001**, *71*, 233–292.
31. Ma, L.; Nielsen, D.C.; Ahuja, L.R.; Malone, R.W.; Saseendran, S.A.; Rojas, K.W.; Hanson, J.D.; Benjamin, J.G. Evaluation of RZWQM under Various Irrigation Levels in Eastern Colorado. *Trans. ASAE* **2003**, *46*, 39–49.
32. Ma, L.; Hook, J.; Wauchope, R. Evapotranspiration Predictions: A Comparison among Gleams, Opus, Przm-2, and RZWQM Models in a Humid and Thermic Climate. *Agric. Syst.* **1999**, *59*, 41–55. [[CrossRef](#)]
33. Ma, L.; Ahuja, L.; Islam, A.; Trout, T.; Saseendran, S.; Malone, R. Modeling Yield and Biomass Responses of Maize Cultivars to Climate Change under Full and Deficit Irrigation. *Agric. Water Manag.* **2017**, *180*, 88–98. [[CrossRef](#)]
34. Ma, L.; Malone, R.; Jaynes, D.; Thorp, K.; Ahuja, L. Simulated Effects of Nitrogen Management and Soil Microbes on Soil Nitrogen Balance and Crop Production. *Soil Sci. Soc. Am. J.* **2008**, *72*, 1594–1603. [[CrossRef](#)]
35. Malone, R.W.; Ma, L.; Heilman, P.; Karlen, D.L.; Kanwar, R.S.; Hatfield, J.L. Simulated N Management Effects on Corn Yield and Tile-Drainage Nitrate Loss. *Geoderma* **2007**, *140*, 272–283. [[CrossRef](#)]
36. Monteith, J.L. Evaporation and Environment. *Symp. Soc. Exp. Biol.* **1965**, *19*, 4.
37. Nielsen, D. and A. Halvorson. Nitrogen Fertility Influence on Water Stress and Yield of Winter Wheat. *Agron. J.* **1991**, *83*, 1065–1070. [[CrossRef](#)]
38. Nimah, M.; Hanks, R. Model for Estimating Soil Water, Plant, and Atmospheric Interrelations: I. Description and Sensitivity. *Soil Sci. Soc. Am. J.* **1973**, *37*, 522–527. [[CrossRef](#)]
39. Novoa, R.; Loomis, R. Nitrogen and Plant Production. *Plant Soil* **1981**, *58*, 177–204. [[CrossRef](#)]
40. Oweis, T.; Zhang, H.; Pala, M. Water use efficiency of rainfed and irrigated bread wheat in a Mediterranean environment. *Agron. J.* **2000**, *92*, 231–238. [[CrossRef](#)]
41. Raun, W.R.; Johnson, G.V. Improving Nitrogen Use Efficiency for Cereal Production. *Agron. J.* **1999**, *91*, 357–363. [[CrossRef](#)]
42. Reynolds, W.D.; Elrick, D.E. A Method for Simultaneous In Situ Measurement in the Vadose Zone of Field-Saturated Hydraulic Conductivity, Sorptivity and the Conductivity-Pressure Head Relationship. *Groundw. Monit. Remediat.* **1986**, *6*, 84–95. [[CrossRef](#)]
43. Ritchie, J.; Johnson, B. Soil and Plant Factors Affecting Evaporation. *Agronomy* **1990**, *11*, 363–390. [[CrossRef](#)]
44. Rudnick, D.R.; Irmak, S.; Djaman, K.; Sharma, V. Impact of irrigation and nitrogen fertilizer rate on soil water trends and maize evapotranspiration during the vegetative and reproductive periods. *Agric. Water Manag.* **2017**, *191*, 77–84. [[CrossRef](#)]
45. Sadras, V.O.; Hayman, P.T.; Rodriguez, D.; Monjardino, M.; Bielich, M.; Unkovich, M.; Mudge, B.; Wang, E. Interactions between water and nitrogen in Australian cropping systems: Physiological, agronomic, economic, breeding and modeling perspectives. *Crop Pasture Sci.* **2016**, *67*, 1019–1053. [[CrossRef](#)]
46. Saseendran, S.; Nielsen, D.; Ma, L.; Ahuja, L.; Halvorson, A. Modeling Nitrogen Management Effects on Winter Wheat Production Using RZWQM and CERES-Wheat. *Agron. J.* **2004**, *96*, 615–630. [[CrossRef](#)]
47. Saseendran, S.; Ahuja, L.; Ma, L.; Nielsen, D.; Trout, T.; Andales, A.; Chávez, J.; Ham, J. Enhancing the Water Stress Factors for Simulation of Corn in RZWQM2. *Agron. J.* **2014**, *106*, 81–94. [[CrossRef](#)]
48. Saseendran, S.; Ahuja, L.R.; Ma, L.; Trout, T. Modeling for Best Management of the Effects of Irrigation Frequencies, Initial Water, and Nitrogen on Corn. In *Practical Applications of Agricultural System Models to Optimize the Use of Limited Water*; Ahuja, L.R., Ma, L., Lascano, R.J., Eds.; Advances in Agricultural Systems Modeling; John Wiley & Sons: Hoboken, NJ, USA, 2014; Volume 5, pp. 25–52.
49. Sexton, B.; Moncrief, J.; Rosen, C.; Gupta, S.; Cheng, H. Optimizing Nitrogen and Irrigation Inputs for Corn Based on Nitrate Leaching and Yield on a Coarse-Textured Soil. *J. Environ. Qual.* **1996**, *25*, 982–992. [[CrossRef](#)]
50. Shaffer, M.J.; Ma, L.; Hansen, S. *Modeling Carbon and Nitrogen Dynamics for Soil Management*; CRC Press: Boca Raton, FL, USA, 2001.
51. Shahadha, S.S.; Wendroth, O.; Zhu, J.; Walton, J. Can measured soil hydraulic properties simulate field water dynamics and crop production? *Agric. Water Manag.* **2019**, *223*, 105661. [[CrossRef](#)]
52. Shuttleworth, W.J.; Wallace, J. Evaporation from Sparse Crops—an Energy Combination Theory. *Q. J. R. Meteorol. Soc.* **1985**, *111*, 839–855. [[CrossRef](#)]
53. Shuttleworth, W.J.; Gurney, R.J. The Theoretical Relationship between Foliage Temperature and Canopy Resistance in Sparse Crops. *Q. J. R. Meteorol. Soc.* **1990**, *116*, 497–519. [[CrossRef](#)]

54. Si, Z.; Zain, M.; Mehmood, F.; Wang, G.; Gao, Y.; Duan, A. Effects of nitrogen application rate and irrigation regime on growth, yield, and water-nitrogen use efficiency of drip-irrigated winter wheat in the North China Plain. *Agric. Water Manag.* **2020**, *231*, 106002. [[CrossRef](#)]
55. Singh, A.K.; Tripathy, R.; Chopra, U.K. Evaluation of CERES-Wheat and CropSyst models for water—Nitrogen interactions in wheat crop. *Agric. Water Manag.* **2008**, *95*, 776–786. [[CrossRef](#)]
56. Smith, R.; Barrs, H.; Fischer, R. Inferring Stomatal Resistance of Sparse Crops from Infrared Measurements of Foliage Temperature. *Agric. For. Meteorol.* **1988**, *42*, 183–198. [[CrossRef](#)]
57. Srivastava, R.K.; Panda, R.K.; Chakraborty, A.; Halder, D. Quantitative estimation of water use efficiency and evapotranspiration under varying nitrogen levels and sowing dates for rainfed and irrigated maize. *Theor. Appl. Climatol.* **2020**, *139*, 1385–1400. [[CrossRef](#)]
58. Szeicz, G.; Long, I. Surface Resistance of Crop Canopies. *Water Resour. Res.* **1969**, *5*, 622–633. [[CrossRef](#)]
59. Wang, Z.; Qi, Z.; Xue, L.; Bukovsky, M.; Helmers, M.J. Modeling the Impacts of Climate Change on Nitrogen Losses and Crop Yield in a Subsurface Drained Field. *Clim. Chang.* **2015**, *129*, 323–335. [[CrossRef](#)]
60. Yang, Y.; Wendroth, O.; Walton, R.J. Field-Scale Bromide Leaching as Affected by Land Use and Rain Characteristics. *Soil Sci. Soc. Am. J.* **2013**, *77*, 1157–1167. [[CrossRef](#)]
61. Yu, Q.; Saseendran, S.A.; Ma, L.; Flerchinger, G.N.; Greenand, T.R.; Ahuja, L.R. Modeling a Wheat–Maize Double Cropping System in China Using Two Plant Growth Modules in RZWQM. *Agric. Syst.* **2006**, *89*, 457–477. [[CrossRef](#)]